HHS Public Access

Author manuscript

Lab Invest. Author manuscript; available in PMC 2016 September 19.

Published in final edited form as:

Lab Invest. 2016 April ; 96(4): 459–467. doi:10.1038/labinvest.2015.158.

Spectrally Encoded Confocal Microscopy (SECM) for Diagnosing of Breast Cancer in Excision and Margin Specimens

Elena F. Brachtel[1], **Nicole B. Johnson**[2], **Amelia E. Huck**[1], **Travis L. Rice-Stitt**[1], **Mark G. Vangel**[3,4], **Barbara L. Smith**[5], **Guillermo J. Tearney**[1,6,7], and **Dongkyun Kang**[6,*]

[1]Department of Pathology, Massachusetts General Hospital

[2]Department of Pathology, Beth Israel Deaconess Medical Center

[3]Department of Radiology, Massachusetts General Hospital

[4]Biostatistics Center, Massachusetts General Hospital

[5]Gillette Center for Women's Cancers and Department of Surgery, Massachusetts General Hospital

[6]Wellman Center for Photomedicine, Massachusetts General Hospital

[7]Harvard-MIT division of Health Sciences and Technology

Abstract

A large percentage of breast cancer patients treated with breast conserving surgery need to undergo multiple surgeries due to positive margins found during post-operative margin assessment. Carcinomas could be removed completely during the initial surgery and additional surgery avoided if positive margins can be determined intra-operatively. Spectrally-encoded confocal microscopy (SECM) is a high-speed reflectance confocal microscopy technology that has a potential to rapidly image the entire surgical margin at sub-cellular resolution and accurately determine margin status intra-operatively. In this paper, in order to test feasibility of using SECM for intra-operative margin assessment, we have evaluated the diagnostic accuracy of SECM for detecting various types of breast cancers. Forty-six surgically-removed breast specimens were imaged with a SECM system. Side-by-side comparison between SECM and histologic images showed that SECM images can visualize key histomorphologic patterns of normal/benign and malignant breast tissues. Small (500 μm × 500 μm) spatially-registered SECM and histologic images (n=124 for each) were diagnosed independently by three pathologists with expertise in breast pathology. Diagnostic accuracy of SECM for determining malignant tissues was high, average sensitivity of 0.91, specificity of 0.93, positive predictive value of 0.95, and negative predictive value of 0.87. Intra-observer agreement and inter-observer agreement for SECM were also high, 0.87 and 0.84, respectively. Results from this study suggest that SECM may be developed into an intra-operative margin assessment tool for guiding breast cancer excisions.

*Corresponding author: Dongkyun Kang, 40 Blossom St. BAR802, Boston, MA 02114, dkang@mgh.harvard.edu, Phone: 617-726-1699, Fax: 617-726-4103.

Disclosure: Drs. Tearney and Kang are inventors of patents and patent applications on the spectrally encoded confocal microscopy technology described in this manuscript. These patents and patent applications are not currently licensed.

Breast cancer excision followed by radiation therapy is a standard breast-conserving therapy for early-stage invasive breast cancers. During the breast excision procedure, primary tumor is surgically removed with a rim of uninvolved breast tissue to allow for negative margins.[1] While breast excision generally provides a better cosmetic outcome and causes less morbidity than mastectomy, it carries a risk of leaving residual tumor behind in the patient, which can cause local recurrence of the breast cancer. An unacceptably large percentage of lumpectomy patients, ~20 to 40 %, are found to have positive margins upon post-operative histologic assessment of the surgical specimen. [2–4] These patients are required to undergo additional surgeries, which pose unnecessary physical and psychological burdens on the patients and an economic burden on the health care system. A few intra-operative margin assessment methods, including frozen section analysis[5,6] and touch preparation analysis [7,8], are used in some institutions and have been shown to reduce the need for additional surgeries. However, these methods are not widely utilized partly because of technical limitations, sampling bias and the requirement of specialist interpretation.

Optical imaging technologies hold great promises for intra-operative margin assessment applications since they can examine optical properties and/or histomorphologic features of freshly excised tissues without the need for frozen section or other tissue preparations. Optical spectroscopy technologies have previously been evaluated for determining margin status intra-operatively. Reflectance spectroscopy measures scattering and absorption properties of freshly excised breast tissues, which can be used to differentiate between benign and malignant patterns. Several studies of imaging breast specimens with reflectance spectroscopy showed that it can detect positive margins with high accuracy.[9–14] Raman spectroscopy can obtain quantitative chemical information of breast tissue, which can be used to distinguish cancerous tissues from normal/benign tissues. Previous studies have shown that Raman spectroscopy can provide high diagnostic accuracy for detecting malignant breast tissues. [15,16]

Optical microscopy technologies have higher resolution than aforementioned optical spectroscopy technologies and might have an advantage in detecting small or infiltrating tumors. Optical coherence tomography (OCT) visualizes architectural differences between normal and malignant tissues and has been shown to determine margin status with high accuracy.[17] OCT technology with cellular resolution, termed optical coherence microscopy (OCM), has also been shown to accurately determine margin status.[18] Fluorescence confocal microscopy (FCM) in conjunction with topical administration of 0.01% proflavine can visualize nuclear details of breast tissues and has been found to accurately diagnose neoplastic tissues.[19] A nonlinear microscopy approach, where two-photon microscopy (TPM) is used to visualize nuclei and second harmonic generation (SHG) microscopy is used to visualize collagens, can generate images that appear similar to histologic images and provide high diagnostic accuracy.[20] Reflectance confocal microcopy (RCM), when used with topical administration of 5% acetic or citric acid, has been shown to visualize nuclear features of various breast tissue types. [21,22] While these optical microscopy technologies show a potential capability for accurately determining margin status intra-operatively, imaging speed needs to be sufficiently high to examine the entire surgical margin within a short procedural time and subsequently provide comprehensive margin information.

Spectrally-encoded confocal microscopy (SECM) is a high-speed RCM technology that has a potential to rapidly image the entire surgical specimen at sub-cellular resolution. SECM uses a diffraction grating to encode a line field of view (FOV) with wavelength. [23] The spectral encoding enables line imaging of the tissue without using any beam scanning mechanism and therefore can increase the imaging speed of RCM significantly. Utilizing a high-speed wavelength-swept source (repetition rate = 100 kHz) and a fast detector unit, SECM was previously demonstrated to rapidly image a human esophageal tissue over an area of 1 cm^2 in 15 seconds.[24] When used during breast cancer surgery, the high speed of SECM could enable the surface of an entire surgical specimen to be rapidly imaged. SECM images can then be used to visually evaluate the margin status. While SECM is expected to visualize key histomorphologic features associated with normal/benign and malignant breast tissues as previous RCM studies have shown, its diagnostic accuracy needs to be confirmed before it can be used for clinical intra-operative applications.

In this study, we evaluated the SECM diagnostic accuracy in determining malignant breast tissues. Surgically-removed breast specimens were imaged with a SECM system. SECM images were compared with corresponding histologic images to identify histomorphologic features visualized in SECM images. Diagnostic accuracy of SECM was evaluated in comparison with the gold standard histologic diagnoses. Intra- and inter-observer agreements were also evaluated.

Methods and Methods

SECM system

We have used a SECM system that was previously developed for imaging gastroesophageal biopsy tissues.[25,26] A schematic of the SECM system is shown in Fig. 1. Light from a custom wavelength-swept source (repetition rate = 5 kHz; central wavelength = 1320 nm; bandwidth = 70 nm) was collimated by a collimation lens (OZ optics; f = 11 mm) and diffracted by a transmission grating (Wasatch Photonics; groove density = 1100 lines/mm). Diffracted light was delivered to the objective lens by relay optics (magnification = 2.4). A high-NA objective lens (UPlanApo/IR 60×, Olympus; NA = 1.2; water immersion) was used to focus the light on the tissue. Light reflected from the breast tissue was collected by the objective lens and travelled back to the beam splitter. Half of the light was reflected at the beam splitter and coupled into a multi-mode fiber and then to a photo detector. The SECM system had lateral resolution of 1.3 μm and axial resolution of 2.4 μm. The width of the spectrally-encoded line was 115 μm. Large-area SECM images of the tissue were acquired by raster-scanning the tissue relative to the spectrally-encoded line using a two-axis motorized translation stage (Nanomover 11NCM001, Melles Griot). Imaging depth was changed by translating the objective lens with a piezoelectric transducer (PZT) actuator (8302, New Port).

Breast tissue imaging

We acquired and imaged breast tissues under a Partners Healthcare IRB-approved protocol (Protocol # 2011P001417). Breast tissues were obtained from the Massachusetts General Hospital (MGH) surgical pathology laboratory directly after the tissues were removed from

the patients. After gross examination and diagnostic sampling of a mastectomy or a breast excision specimen, selected fresh breast tissue fragments (size = ~ 0.5–2 cm) were sampled and transferred to the SECM system. Breast tissues were de-identified and each tissue was assigned with a unique study number. A total of 46 samples were obtained from 35 surgical specimens.

Each breast tissue was treated with 5% acetic acid to enhance nuclear contrast.[21,22] The breast tissue was then placed onto the translation stage underneath the objective lens. Large-area SECM images (size = 4 × 2 mm^2 - 10 × 4.8 mm^2) were obtained from several focal planes (number of focal planes = 2–10) covering imaging depth range of 0 – 200 μm. SECM imaging time ranged from 10 to 15 minutes. Once SECM imaging was completed, the tissue was then prepared as hematoxylin and eosin (H&E)-stained histologic slides per standard procedure. The tissue was cut *en face* to achieve good spatial registration between SECM and histologic images. Histologic slides were scanned by a whole slide scanner (Nanozoomer, Hamamatsu; 20× objective lens with NA of 0.75; scanning resolution = 0.46 μm). Digital images of the histologic slides were used for image analysis.

Evaluation of diagnostic accuracy

SECM and histologic images obtained from the same breast tissue were compared at various magnifications (Fig. 2). SECM images were displayed with an inverted color map, which made highly-scattering features such as cell nuclei appear dark and surrounding tissue bright. An image reader (DK) who was blinded to the histologic diagnoses reviewed multiple SECM images obtained from different focal planes and determined the focal plane that had highest spatial correlation to the histologic image. The image reader then identified small regions (size of each region = 500 μm × 500 μm) that exhibited similar microscopic features between SECM and histologic images and saved the SECM and histologic regions as uncompressed TIFF and JPEG image files, respectively. We used JPEG file type for histologic images since the whole slide images were saved with JPEG compression. Each JPEG image was displayed as a 15.9 cm × 15.9 cm square (700 pixels × 700 pixels) on a 13.3” screen (Mac Book Pro, Apple). At this display condition, there was not any noticeable image degradation. A total of 154 pairs of registered SECM and histologic images were generated.

The 154 histologic images were then reviewed by a senior breast pathologist (EFB), who made diagnoses on each histologic image into either one of the six normal/benign categories (adipose, fibrous, ducts/glands, inflammation, proliferative, unspecified normal/benign) or one of the seven malignant categories (invasive ductal carcinoma (IDC), invasive lobular carcinoma (ILC), unspecified invasive carcinoma (IC), ductal carcinoma in situ (DCIS), lobular carcinoma in situ (LCIS), unspecified carcinoma in situ (CIS), unspecified malignant). Diagnoses by the senior pathologist were used as the gold standard during the diagnostic accuracy evaluation. After completing the gold standard diagnoses, the senior pathologist reviewed SECM images in comparison with corresponding histologic images to identify histomorphologic features visualized in SECM images.

Three pathologists with expertise in breast pathology (NBJ, AEH, TLRS), who were blinded to the prior diagnoses by the senior pathologist, were trained to read SECM images. During

the training session, each pathologist was presented with 30 pairs of SECM and histologic images side by side along with a written summary of histomorphologic features visualized in SECM images. After the training session, each pathologist reviewed 124 SECM images and prospectively rendered diagnosis for each SECM image as one of the six normal/benign or one of the seven malignant tissue categories listed above. The three pathologists also made diagnoses on 124 corresponding histologic images. Each pathologist conducted two sessions of SECM image review and two sessions of histologic image review to determine intra-observer agreement. In each image review session, images were presented in a random order. There was at least a 24-hour washout period between image review sessions. Sensitivity and specificity for determining malignant tissues for each pathologist and each image review session were evaluated in comparison with the gold standard. Positive predictive value (PPV), negative predictive value (NPV), and accuracy were also calculated. Intra-observer agreement was evaluated by calculating Cohen's kappa for each pathologist and each modality. Inter-observer agreement was calculated by pairwise comparison, where Cohen's kappa was calculated between two pathologists' diagnoses. Six kappa values were generated for each of the SECM and histologic diagnoses. Two-tailed p-values were calculated to compare sensitivity, specificity, intra-observer agreement, and inter-observer agreement measurements between SECM and histologic diagnoses. Logistic regression was used to calculate overall difference in sensitivity and specificity between SECM and histology.

Results

SECM image of normal/benign breast tissue

In SECM images, the structures appear on a gray scale in black and white, while histologic images stained by H&E show cytoplasm and collagenous tissue as pink and nuclei as blue. Representative SECM and histologic images of normal/benign breast tissues are shown in Fig. 3. In an SECM image of fibrous tissue (Fig. 3a), collagen of the fibrous tissue appears as a dark wavy structure that is similar to that of the corresponding histologic image (Fig. 3b). Adipose cells (asterisks) are visualized as bright circles in an SECM image of the fat tissue (Fig. 3c). The fat cells also exhibit crystalline-appearing structures centrally. An SECM image of the benign ducts and glands (Fig. 3e) shows several regularly-shaped glands. Each gland is clearly delineated by cell nuclei (arrows in inset, Fig. 3e) that are similar in appearance to the nuclei seen in the corresponding histologic image (Fig. 3f). SECM and histologic images of inflamed tissue (Figs. 3g and h) both show numerous lymphocytes.

SECM image of malignant breast tissue

Representative SECM and histologic images of malignant breast tissues are shown in Fig. 4. In both SECM and histologic images of DCIS (Figs. 4a and b), a cribriform architecture (asterisks) is clearly shown, and tumor cells are well contained inside the ductal membrane (dotted lines). In Figs. 4c and d, low-grade IDC is visualized with small irregularly-shaped glands (dotted lines) invading surrounding stroma. An SECM image of high-grade IDC (Fig. 4e) enables the visualization of diffuse growth of tumor cells with virtually no stroma; comparable features are also seen in the corresponding histologic image (Fig. 4f). In SECM

and histologic images of ILC (Figs. 4g and h), small and dyshesive tumor cells (arrows) are scattered between normal-looking stroma.

Diagnostic accuracy evaluation

Among the 124 pairs of SECM and histologic images used during diagnostic accuracy evaluation, 49 were benign/normal and 75 were malignant per gold standard. Time required for rendering diagnoses on 124 images during each image review session was from 15–20 minutes for both SECM and histology.

Sensitivity and specificity evaluation results are summarized in Table 1. Sensitivity for SECM was high, ranging from 0.89 (95% CI: 0.8–0.95) to 0.95 (0.87–0.98), and average sensitivity was 0.91. SECM specificity was also high, 0.88 (0.76–0.94) to 0.98 (0.89–1), and average value was 0.93. Histology sensitivity ranged from 0.85 (0.76–0.92) to 1 (0.95–1), and specificity from 0.96 (0.86–0.99) to 1 (0.93–1). Average sensitivity and specificity for SECM were slightly lower than those for histology. There were statistically-significant differences ($p<0.05$) in two of the sensitivity measurements and two of the specificity measurements, highlighted in Table 1. The other four sensitivity measurements and four specificity measurements did not show statistically-significant differences. Logistic regression showed that overall sensitivity and specificity of SECM were significantly different from those of histology, p-values less than 0.01 and 0.001, respectively. Average positive predictive value (PPV) for SECM was 0.95, and negative predictive value (NPV) 0.87. Average PPV and NPV for histology were 0.99 and 0.94, respectively. Average diagnostic accuracy for SECM was 0.92, and average accuracy for histology was 0.97.

Intra-observer agreement evaluation results are summarized in Table 2. Intra-observer agreement for SECM was high, ranging from 0.82 (0.72–0.92) to 0.92 (0.84–0.99), and average kappa value was 0.87. Similarly, intra-observer agreement for histology was high, 0.84 (0.74–0.93) to 0.98 (0.95–1), with average of 0.92. One of three kappa value comparisons showed a statistically-significant difference.

Table 3 shows summary of inter-observer agreement evaluation results. Inter-observer agreement for SECM diagnoses was high, 0.77 (0.66–0.88) to 0.87 (0.78–0.96), with an average of 0.84. Histology also showed high inter-observer agreement, 0.79 (0.68–0.90) to 0.97 (0.92–1.00), with an average of 0.90. There was one kappa value comparison that showed a statistically-significant difference between SECM and histology.

Discussion on discrepant cases

There were four cases where more than half of the six SECM diagnoses were incorrect while more than half of the six histologic diagnoses were correct. Two of these cases were SECM malignant and histology normal/benign and showed similar histomorphologic features. One of these cases is shown in Figs. 5a and b. The gold standard diagnosis was ducts/glands. In SECM image (Fig. 5a), there are scattered areas where cell nuclei are not reliably visualized, which made it challenging to delineate boundary of each acinus and made the SECM image appear similar to invasive carcinoma with no stroma. The other two cases were SECM normal/benign and histology malignant and exhibited similar microscopic features. Figs. 5c and d show SECM and histologic images for one of these cases. The gold standard diagnosis

for these images was ILC. SECM image (Fig. 5c) appears to have poor resolution: cell nuclei in the stroma are not well visualized (dotted line) and boundaries of fat cells are not clearly distinguished (right side and bottom).

Discussion

Results from this study show that sensitivity and specificity of SECM for detecting malignant breast tumors are high. SECM sensitivity and specificity are similar to the sensitivity and specificity previously reported for other optical microscopy technologies.[19,20] Study results also show that intra- and inter-observer agreements for SECM are high. With the high diagnostic accuracy demonstrated in this paper and fast imaging speed shown in our previous work[24], SECM will uniquely enable microscopic imaging of the entire breast excision specimens in a short imaging time and provide accurate margin status during the surgery. Real-time feedback regarding the margin status will be used to conduct additional re-resections to finally achieve negative margin during the initial surgery, which can obviate the need for additional surgeries.

Average SECM sensitivity and specificity were lower than average histologic sensitivity and specificity. SECM occasionally produced poor image quality for a few images (Figs. 5a and c). If we exclude the four poor-image-quality cases described in the results section, average SECM sensitivity and specificity become 0.94 and 0.97, respectively, and differences in average sensitivity and specificity between SECM and histology become statistically insignificant (p values = 0.10 and 0.12, respectively). SECM images obtained from superficial regions visualized cellular features in a similar manner to histologic images even though the lateral resolution was worse for SECM than the whole slide scanner, 1.3 μm versus 0.43 μm. At large imaging depths, the effective resolution of SECM was significantly degraded due to light scattering and optical aberrations, which resulted in poor image quality as exemplified in Figs. 5a and c. This study has been helpful in educating us about the difficulties of diagnosing SECM images that are too deep below the surface of the tissue. These findings suggest that during intra-operative imaging, SECM images should be obtained from a superficial focal plane, where resolution is retained and diagnostic accuracy is likely to be higher.

There were several limitations in this study: (1) Diagnostic accuracy was tested by reviewing small images. Accuracy of determining margin status by reviewing a large SECM image of the entire surgical specimen still needs to be evaluated. (2) Similarly, the amount of time needed to review a large SECM image at various magnifications and determine margin status needs to be studied. (3) Breast samples were resected by scalpels from mastectomy or excision specimens and did not have cautery artifacts. Effects of cautery artifacts on SECM diagnostic accuracy are not known yet. (4) Histologic margin assessment is generally conducted on cross sections of the tissue, while SECM margin assessment is conducted on *en face* planes. Clinical implication of the *en face* SECM margin status has not been studied. (5) Margin width information is not obtained in SECM due to *en face* manner of SECM imaging and its limited imaging depth, typically around 200 μm. Recent guideline on margins for breast-conserving surgery found that while a negative margin lowers risk of local recurrence, there is no statistically significant correlation between margin width and

reduction of local recurrence rate.[1] We therefore expect that lack of margin width information will not limit SECM's capability to guiding breast cancer excision. This hypothesis, however, will need to be tested in future clinical studies. (6) Study samples mainly included common breast cancers but did not have more complex diseases, including atypical intraductal proliferations, small foci of carcinoma, lymphatic vessel invasion, and microinvasive carcinoma in a background of extensive DCIS. Diagnostic accuracies for these complex diseases need to be evaluated.

SECM still needs technical improvements on following items before it can be fully utilized for clinical intra-operative applications: (1) While the fast SECM imaging speed (100 kHz line rate[24]) will enable imaging of the entire excision specimen (typical size = ~30cm^2) in a short time (7.5 minutes), faster imaging speed might be needed to allow for more time to review SECM images. We can increase the imaging speed further by using a higher-rate swept source (several MHz)[27,28] and higher speed detectors and digitizer systems. (2) Adequate software needs to be developed for fast image display and navigation to enable intra-operative margin assessment with SECM images. We will develop a fast image display/navigation method that are similar to those used in whole slide imaging (WSI) systems, where original large image with full resolution is converted into a pyramidal structure for rapid image display/navigation. With an adequate image display/navigation software, we expect that time from tissue excision to final SECM margin determination will be similar to turnaround time for WSI-based diagnosis of a frozen section, around 15 minutes[29], since image review time was found to be similar between SECM and histology in this study. (3) An automated tissue type recognition software could be used to further reduce the image review time. The automated software could identify regions that need to be examined by the pathologist. By focusing on these selected regions, the pathologist could complete the image review within a shorter time. Previously, several algorithms were developed to automatically analyze histomorphologic patterns in histologic images of breast tissues. [30,31] We will develop a similar pattern analysis algorithm for SECM breast images. (4) A systematic scanning method needs to be developed to image the entire surface of the breast excision specimen. While development of the scanning method will need to be done in conjunction with end user surgeon and pathologist requirements, at present we suggest the following protocol: 1) For shaved margin specimens, when oriented, the patient-side surface will be comprehensively imaged, whereas if not oriented, both sides will be imaged, 2) For lumpectomy specimens, the SECM device will be configured to scan in three-dimensions over the surface of the specimen and registered with orientation landmarks provided by the surgeon.

In the future, we will develop an intra-operative SECM system that can be used to study and address the aforementioned technical challenges. We will then conduct a clinical study of utilizing the intra-operative SECM system in guiding breast cancer excision. In this future study, we will image entire excision specimens with SECM, determine margin status, and resect additional tissues based on the SECM margin status along with findings from other intra-operative imaging modalities. From this clinical study, we will be able to evaluate effectiveness of SECM for reducing the need for additional surgeries.

Acknowledgments

Authors thank Mr. Jeonghyun Lee for his help on digitizing histology slides. Authors also thank the MGH surgical pathology unit for their help on procuring surgical breast tissues. Dr. Huck is currently with Saint Barnabas Medical Center (Livingston, NJ). This work was supported by Center for Integration of Medicine and Innovative Technology (CIMIT) under U.S. Army Medical Research Acquisition Activity Cooperative Agreement (W81XWH-09-2-0001). The information contained herein does not necessarily reflect the position or policy of the Government, and no official endorsement should be inferred. This work was conducted with support from Harvard Catalyst | The Harvard Clinical and Translational Science Center (National Center for Research Resources and the National Center for Advancing Translational Sciences, National Institutes of Health Award UL1 TR001102) and financial contributions from Harvard University and its affiliated academic healthcare centers. The content is solely the responsibility of the authors and does not necessarily represent the official views of Harvard Catalyst, Harvard University and its affiliated academic healthcare centers, or the National Institutes of Health.

References

1. Moran MS, Schnitt SJ, Giuliano AE, et al. Society of Surgical Oncology–American Society for Radiation Oncology consensus guideline on margins for breast-conserving surgery with whole-breast irradiation in stages I and II invasive breast cancer. Int J Radiation Oncol Biol Phys. 2014; 88:553–564.
2. McCahill LE, Single RM, Aiello Bowles EJ, et al. Variability in reexcision following breast conservation surgery. JAMA. 2012; 307:467–475. [PubMed: 22298678]
3. Morrow M, Jagsi R, Alderman AK, et al. Surgeon recommendations and receipt of mastectomy for treatment of breast cancer. JAMA. 2009; 302:1551–1556. [PubMed: 19826024]
4. Coopey SB, Buckley JM, Smith BL, et al. Lumpectomy cavity shaved margins do not impact re-excision rates in breast cancer patients. Annals of surgical oncology. 2011; 18:3036–3040. [PubMed: 21947583]
5. Boughey JC, Hieken TJ, Jakub JW, et al. Impact of analysis of frozen-section margin on reoperation rates in women undergoing lumpectomy for breast cancer: evaluation of the National Surgical Quality Improvement Program data. Surgery. 2014; 156:190–197. [PubMed: 24929768]
6. Uecker JM, Bui EH, Foulkrod KH, et al. Intraoperative assessment of breast cancer specimens decreases cost and number of reoperations. The American surgeon. 2011; 77:342–344. [PubMed: 21375848]
7. Esbona K, Li Z, Wilke LG. Intraoperative imprint cytology and frozen section pathology for margin assessment in breast conservation surgery: a systematic review. Annals of surgical oncology. 2012; 19:3236–3245. [PubMed: 22847119]
8. D'Halluin F, Tas P, Rouquette S, et al. Intra-operative touch preparation cytology following lumpectomy for breast cancer: a series of 400 procedures. The Breast. 2009; 18:248–253. [PubMed: 19515566]
9. Sharma V, Shivalingaiah S, Peng Y, et al. Auto-fluorescence lifetime and light reflectance spectroscopy for breast cancer diagnosis: potential tools for intraoperative margin detection. Biomed. Opt. Express. 2012; 3:1825–1840. [PubMed: 22876347]
10. Keller MD, Majumder SK, Kelley MC, et al. Autofluorescence and diffuse reflectance spectroscopy and spectral imaging for breast surgical margin analysis. Lasers in surgery and medicine. 2010; 42:15–23. [PubMed: 20077490]
11. Nachabé R, Evers DJ, Hendriks BH, et al. Diagnosis of breast cancer using diffuse optical spectroscopy from 500 to 1600 nm: comparison of classification methods. Journal of biomedical optics. 2011; 16 087010-087010-087012.
12. Brown JQ, Bydlon TM, Kennedy SA, et al. Optical spectral surveillance of breast tissue landscapes for detection of residual disease in breast tumor margins. PloS one. 2013; 8:e69906. [PubMed: 23922850]
13. Laughney AM, Krishnaswamy V, Rizzo EJ, et al. Scatter spectroscopic imaging distinguishes between breast pathologies in tissues relevant to surgical margin assessment. Clinical Cancer Research. 2012; 18:6315–6325. [PubMed: 22908098]

14. Lue N, Kang JW, Yu C-C, et al. Portable optical fiber probe-based spectroscopic scanner for rapid cancer diagnosis: a new tool for intraoperative margin assessment. PloS one. 2012; 7:e30887. [PubMed: 22303465]
15. Keller MD, Vargis E, de Matos Granja N, et al. Development of a spatially offset Raman spectroscopy probe for breast tumor surgical margin evaluation. Journal of biomedical optics. 2011; 16 077006-077006-077008.
16. Haka AS, Volynskaya Z, Gardecki JA, et al. In vivo Margin Assessment during Partial Mastectomy Breast Surgery Using Raman Spectroscopy. Cancer Research. 2006; 66:3317–3322. [PubMed: 16540686]
17. Nguyen FT, Zysk AM, Chaney EJ, et al. Intraoperative evaluation of breast tumor margins with optical coherence tomography. Cancer research. 2009; 69:8790–8796. [PubMed: 19910294]
18. Assayag O, Antoine M, Sigal-Zafrani B, et al. Large field, high resolution full-field optical coherence tomography: a pre-clinical study of human breast tissue and cancer assessment. Technology in cancer research & treatment. 2014; 13:455–468. [PubMed: 24000981]
19. Dobbs JL, Ding H, Benveniste AP, et al. Feasibility of confocal fluorescence microscopy for real-time evaluation of neoplasia in fresh human breast tissue. Journal of biomedical optics. 2013; 18:106016–106016. [PubMed: 24165742]
20. Tao YK, Shen D, Sheikine Y, et al. Assessment of breast pathologies using nonlinear microscopy. Proceedings of the National Academy of Sciences. 2014; 111:15304–15309.
21. Schiffhauer LM, Boger JN, Bonfiglio TA, et al. Confocal microscopy of unfixed breast needle core biopsies: a comparison to fixed and stained sections. BMC Cancer. 2009; 9:265–265. [PubMed: 19650910]
22. Tilli MT, Cabrera MC, Parrish AR, et al. Real-time imaging and characterization of human breast tissue by reflectance confocal microscopy. Journal of Biomedical Optics. 2007; 12:051901–051910. [PubMed: 17994884]
23. Tearney GJ, Webb RH, Bouma BE. Spectrally encoded confocal microscopy. Optics letters. 1998; 23:1152–1154. [PubMed: 18087457]
24. Schlachter SC, Kang D, Gora MJ, et al. Spectrally encoded confocal microscopy of esophageal tissues at 100 kHz line rate. Biomed. Opt. Express. 2013; 4:1636–1645. [PubMed: 24049684]
25. Kang D, Suter MJ, Boudoux C, et al. Comprehensive imaging of gastroesophageal biopsy samples by spectrally encoded confocal microscopy. Gastrointest Endosc. 2010; 71:35–43. [PubMed: 19922916]
26. Kang D, Suter MJ, Boudoux C, et al. Co-registered spectrally encoded confocal microscopy and optical frequency domain imaging system. Journal of microscopy. 2010; 239:87–91. [PubMed: 20629914]
27. Reznicek L, Klein T, Wieser W, et al. Megahertz ultra-wide-field swept-source retina optical coherence tomography compared to current existing imaging devices. Graefe's Archive for Clinical and Experimental Ophthalmology. 2014; 252:1009–1016.
28. Xu J, Zhang C, Xu J, et al. Megahertz all-optical swept-source optical coherence tomography based on broadband amplified optical time-stretch. Optics letters. 2014; 39:622–625. [PubMed: 24487881]
29. Pantanowitz L, Valenstein PN, Evans AJ, et al. Review of the current state of whole slide imaging in pathology. Journal of pathology informatics. 2011; 2:36. [PubMed: 21886892]
30. Naik, S.; Doyle, S.; Agner, S., et al. Biomedical Imaging: From Nano to Macro, 2008. ISBI 2008. 5th IEEE International Symposium on. IEEE; p. 284-287.
31. Petushi S, Garcia FU, Haber MM, et al. Large-scale computations on histology images reveal grade-differentiating parameters for breast cancer. BMC Medical Imaging. 2006; 6:14. [PubMed: 17069651]

Abbreviations

CIS	carcinoma in situ
DCIS	ductal carcinoma in situ

FCM	fluorescence confocal microscopy
FOV	field of view
H&E	hematoxylin and eosin
IC	invasive carcinoma
IDC	invasive ductal carcinoma
ILC	invasive lobular carcinoma
LCIS	lobular carcinoma in situ
NPV	negative predictive value
OCM	optical coherence microscopy
OCT	optical coherence tomography
PPV	positive predictive value
PZT	piezoelectric transducer
RCM	reflectance confocal microscopy
SECM	spectrally encoded confocal microscopy
SHG	second harmonic generation
TPM	two-photon microscopy

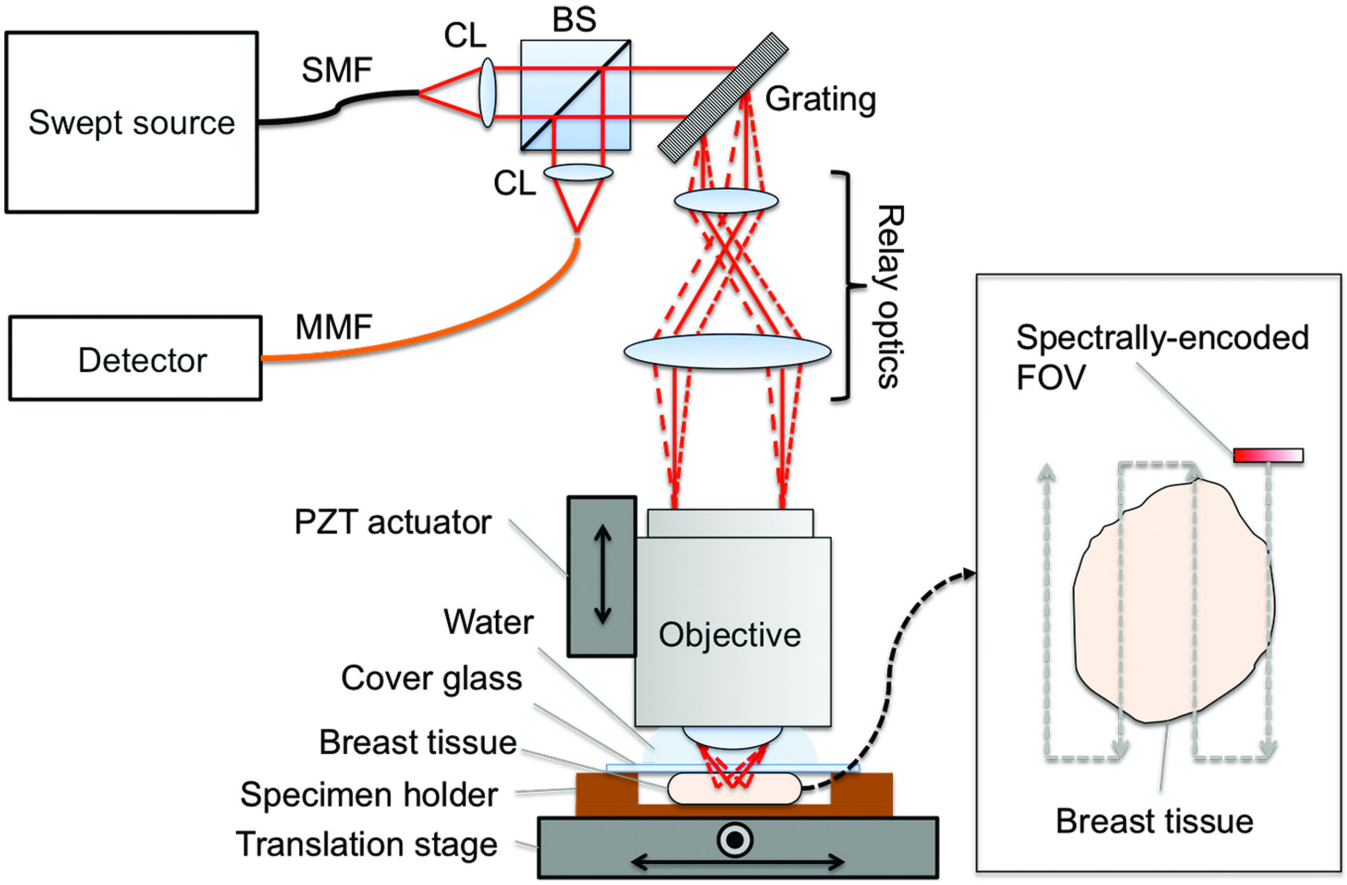

Figure 1.

Schematic of SECM system. BS, beam splitter; CL, collimation lens; FOV, field of viw; MMF, multi-mode fiber; PZT, piezo-electric transducer; SECM, spectrally encoded confocal microscopy; SMF, single-mode fiber.

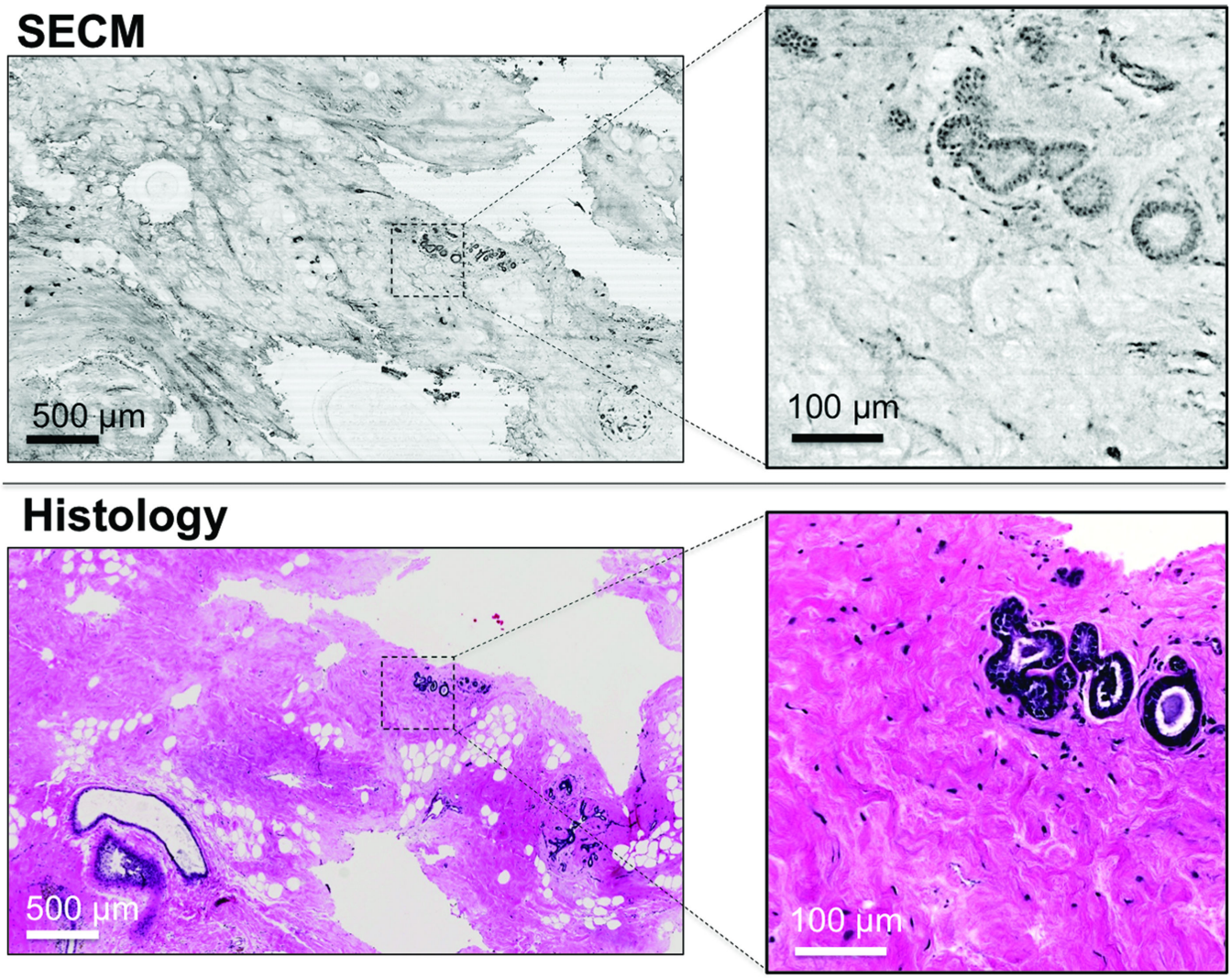

Figure 2.

Representative SECM and histologic images of a breast tissue as overview at low magnification (left) and in high magnification (right) with magnified area in box insert.

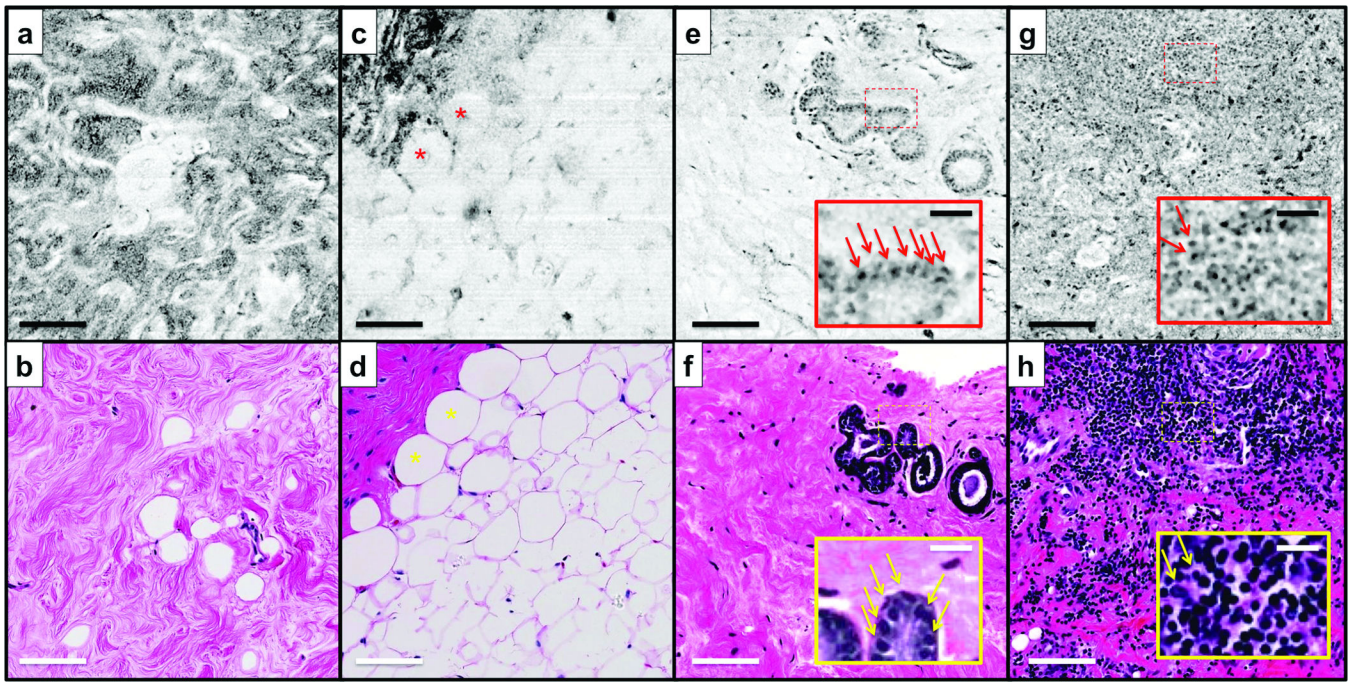

Figure 3.

Representative spectrally encoded confocal microscopy (SECM) and histologic images of normal/benign breast tissues. (a, c, e, and g) SECM images. (b, d, f, and h) Histologic images. (a and b) Fibrous tissue. (c and d) Adipose tissue. (e and f) Benign ducts and glands. (g and h) Inflammation. Asterisks, fat cells; arrows, cell nuclei.

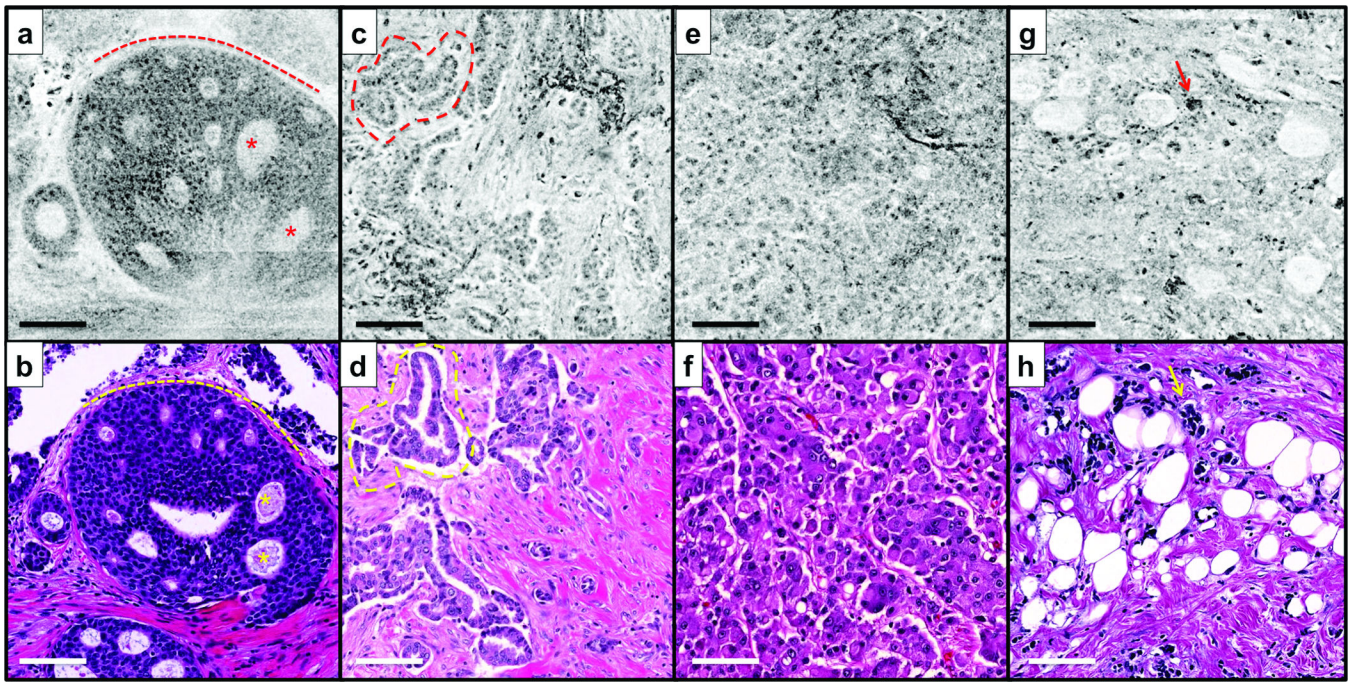

Figure 4.

Representative spectrally encoded confocal microscopy (SECM) and histologic images of malignant breast tissues. (a, c, e, and g) SECM images. (b, d, f, and h) Histologic images. (a and b) Round foci of ductal carcinoma in situ (DCIS). (c and d) Low-grade invasive ductal carcinoma (IDC) with formation of irregular glandular structures. (e and f) High-grade IDC with diffuse sheets of tumor cells. (g and h) Invasive lobular carcinoma (ILC) with individual invasive cells. Asterisks, cribriform architecture; dotted line in a and b, basement membrane; dotted line in c and d, irregularly-shaped glands; arrows, tumor cells.

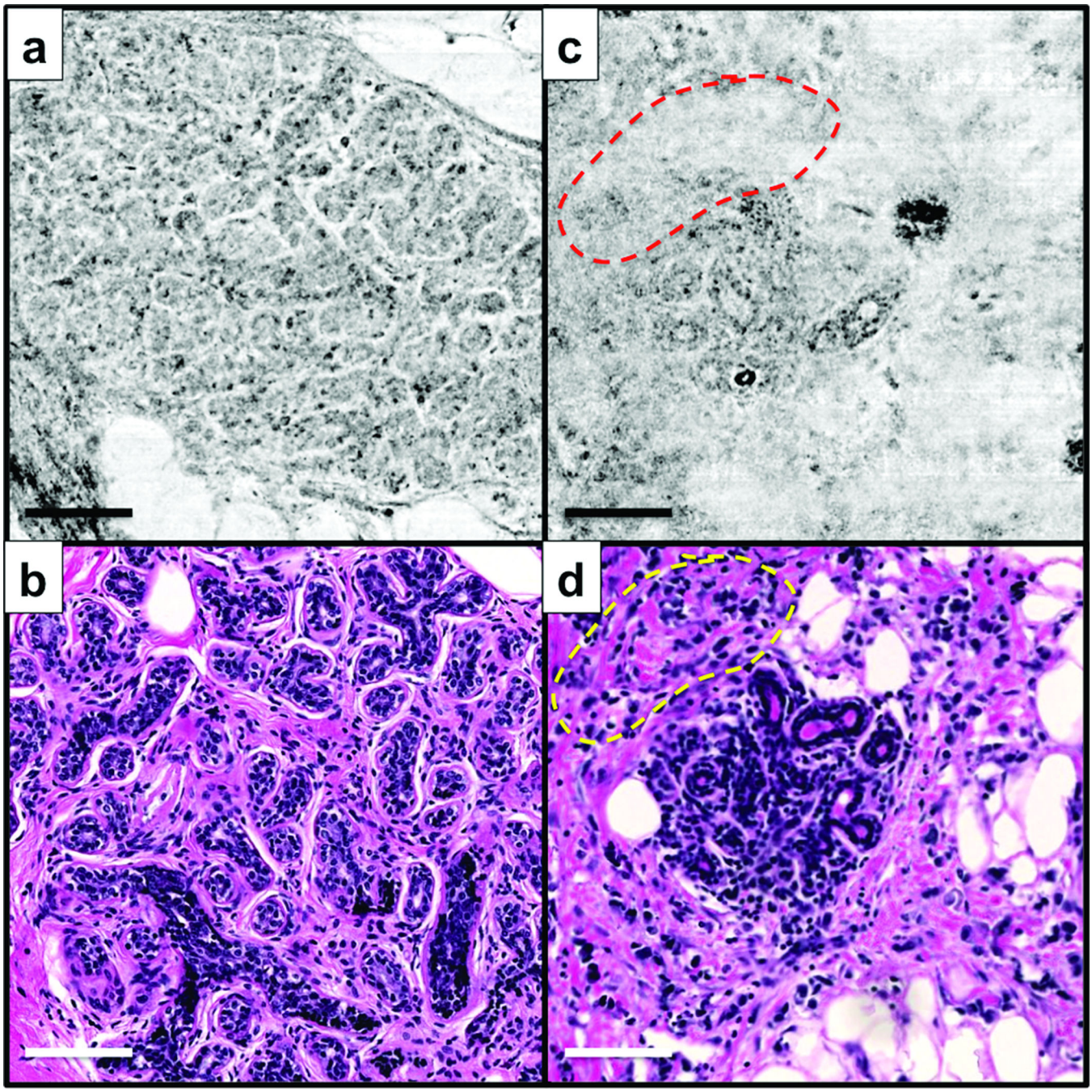

Figure 5.

Representative SECM and histologic images for cases with incorrect SECM diagnoses but correct histologic diagnoses. a and b – ducts/glands; and c and d – ILC. dotted line – area where SECM image failed to clearly visualize cell nuclei in stroma.

Table 1

Sensitivity and specificity test results. Numbers in parenthesis show lower and upper limits of 95% confidence interval. P-values less than 0.05 are highlighted by bold and italic fonts.

	SECM		Histology		p-value	
	Sensitivity	**Specificity**	**Sensitivity**	**Specificity**	**Sensitivity**	**Specificity**
Pathologist 1	0.91 (0.82–0.95)	0.96 (0.86–0.99)	1.00 (0.95–1.00)	0.96 (0.86–0.99)	***0.01***	1.00
	0.89 (0.80–0.95)	0.92 (0.81–0.97)	0.99 (0.93–1.00)	0.96 (0.86–0.99)	***0.01***	0.41
Pathologist 2	0.89 (0.80–0.95)	0.98 (0.89–1.00)	0.85 (0.76–0.92)	1.00 (0.93–1.00)	0.46	0.31
	0.95 (0.87–0.98)	0.92 (0.81–0.97)	0.99 (0.93–1.00)	1.00 (0.93–1.00)	0.17	***0.046***
Pathologist 3	0.91 (0.82–0.95)	0.92 (0.81–0.97)	0.96 (0.89–0.99)	1.00 (0.93–1.00)	0.17	***0.046***
	0.92 (0.84–0.96)	0.88 (0.76–0.94)	0.95 (0.87–0.98)	0.98 (0.89–1.00)	0.51	0.06
Average	**0.91**	**0.93**	**0.96**	**0.98**	***<0.01***	***<0.001***

Lab Invest. Author manuscript; available in PMC 2016 September 19.

Table 2

Intra-observer agreement evaluation results. Numbers in parenthesis show lower and upper limits of 95% confidence interval. P-values less than 0.05 are highlighted by bold and italic fonts.

	SECM	Histology	p-value
Pathologist 1	0.88 (0.80–0.97)	0.98 (0.95–1.00)	***0.03***
Pathologist 2	0.82 (0.72–0.92)	0.84 (0.74–0.93)	0.79
Pathologist 3	0.92 (0.84–0.99)	0.93 (0.87–1.00)	0.72
Average	**0.87**	**0.92**	

Table 3

Inter-observer agreement evaluation results. Numbers in parenthesis show lower and upper limits of 95% confidence interval. P-values less than 0.05 are highlighted by bold and italic fonts.

	SECM	Histology	p-value
Pathologist 1 vs 2	0.80 (0.70–0.91)	0.79 (0.68–0.90)	0.84
	0.83 (0.74–0.93)	0.97 (0.92–1.00)	***0.02***
Pathologist 2 vs 3	0.77 (0.66–0.88)	0.87 (0.78–0.96)	0.17
	0.87 (0.78–0.96)	0.93 (0.87–1.00)	0.23
Pathologist 3 vs 1	0.87 (0.78–0.96)	0.92 (0.84–0.99)	0.41
	0.87 (0.78–0.96)	0.93 (0.87–1.00)	0.24
Average	**0.84**	**0.90**	